Journal of Biomedical Optics

BiomedicalOptics.SPIEDigitalLibrary.org

Influence of multiple scattering and absorption on the full scattering profile and the isobaric point in tissue

Hamootal Duadi
Dror Fixler

SPIE.

Journal of Biomedical Optics 20(5), 056010 (May 2015)

Influence of multiple scattering and absorption on the full scattering profile and the isobaric point in tissue

Hamootal Duadi and Dror Fixler*
Bar Ilan University, Institute of Nanotechnology and Advanced Materials, Faculty of Engineering, Ramat Gan 5290002, Israel

Abstract. Light reflectance and transmission from soft tissue has been utilized in noninvasive clinical measurement devices such as the photoplethysmograph (PPG) and reflectance pulse oximeter. Incident light on the skin travels into the underlying layers and is in part reflected back to the surface, in part transferred and in part absorbed. Most methods of near infrared (NIR) spectroscopy focus on the volume reflectance from a semi-infinite sample, while very few measure transmission. We have previously shown that examining the full scattering profile (angular distribution of exiting photons) provides more comprehensive information when measuring from a cylindrical tissue. Furthermore, an isobaric point was found which is not dependent on changes in the reduced scattering coefficient. The angle corresponding to this isobaric point depends on the tissue diameter. We investigated the role of multiple scattering and absorption on the full scattering profile of a cylindrical tissue. First, we define the range in which multiple scattering occurs for different tissue diameters. Next, we examine the role of the absorption coefficient in the attenuation of the full scattering profile. We demonstrate that the absorption linearly influences the intensity at each angle of the full scattering profile and, more importantly, the absorption does not change the position of the isobaric point. The findings of this work demonstrate a realistic model for optical tissue measurements such as NIR spectroscopy, PPG, and pulse oximetery. [DOI: 10.1117/1.JBO.20.5.056010]

Keywords: light–tissue interaction; photon migration; Monte Carlo simulation; multiple scattering.

Paper 150146R received Mar. 11, 2015; accepted for publication Apr. 27, 2015; published online May 27, 2015.

1 Introduction

Human tissue is one of the most complex optical media since it is nonhomogeneous. Furthermore, its optical properties, such as the absorption coefficient μ_a, the scattering coefficient μ_s, and the anisotropy factor g, are unknown and vary in different types of tissues and physiological states. An understanding of these properties would allow for a noninvasive examination of different physiological parameters, such as blood saturation, blood pressure, blood perfusion, and so on.[1]

Most spectroscopy and tomography methods refer to tissue as a multiple scattering medium.[2–6] However, this assumption is only correct for tissues significantly thicker than the transport mean free path.[7,8] This condition is usually the case in *in vivo* measurements, but not necessarily in pinched tissue, ear lobe or fingertip joint; hence, the role of multiple scattering in specific applications is rarely discussed.

When examining tissue *in vivo*, several diagnostic techniques exist, such as magnetic resonance imaging, computed tomography, and ultrasound. Optical diagnostic techniques have their advantages over these techniques since they are nonionizing, fast, inexpensive, and simple; however, they are limited in penetration depth.[9] Imaging human tissue is restricted to the subsurface (several mm), while diffusion measurements examine deeper tissue layers (up to several cm).[10]

In near infrared (NIR) spectroscopy most methods focus on the volume reflectance from a semi-infinite sample.[11–19] We have previously shown that examining the full scattering profile (angular distribution of exiting photons) gives a more informative measurement from a cylindrical tissue, since it is sensitive to changes in the reduced scattering coefficient (μ_s').[20] Furthermore, an isobaric point, which is not influenced by changes in the reduced scattering coefficient, was found Thus, that the isobaric point is the intersection point of the full scattering profiles for different reduced scattering coefficients. The value of this isobaric point depends on the tissue diameter.[21] By examining the full scattering coefficient for pulse oximetry, we avoid the need for calibration and the need for a two wavelength measurement, as in the conventional method.[22]

Many applications from cylindrical tissues measurements exist, for example, in photoplethysmography (PPG) for calculation of arterial oxygen saturation and heart rate.[23] In PPG, the region being studied is typically the fingertip (about 10 to 15 mm diameter) or earlobe (about 5 mm diameter). Hence, we choose these diameters in our simulations.

The simulation used in this research is a Monte Carlo (MC) simulation which has been previously compared to experimental results in order to verify its validity.[11] The classical MC model of steady-state light transport in multilayered tissues code[17] was not used since it was designed for reflection measurements from a semi-infinite media, and hence, is not suitable for collecting the full scattering profile of a cylindrical tissue.

In this work, we will further investigate the role of multiple scattering and will add the absorption parameter to a cylindrical tissue. First, we will simulate tissue without absorption as a control to find the range in which multiple scattering occurs for

*Address all correspondence to: Dror Fixler, E-mail: Dror.Fixler@biu.ac.il

1083-3668/2015/$25.00 © 2015 SPIE

different tissue diameters. By finding the value and angle of the maximal intensity of the full scattering profile, we will better define the condition for multiple scattering. Next, we will test the role of the absorption coefficient in the attenuation of the full scattering profile, which was previously ignored. We will show that the intensity linearly depends on the scattering coefficient, while the absorption does not change the position of the isobaric point. Furthermore, this linear dependency also exists in multiple scattering, although the slope of this linear relation varies according to the scattering coefficient.

2 Materials and Methods

2.1 *Two-Dimensional Model of Circular Scattering Tissue*

To understand the influence of multiple scattering in different tissue diameters, several simulations were executed on a two-dimensional (2-D) model of a circular tissue cross-section [Fig. 1(a)]. A beam of photons with a waist of $w_0 = 1.5$ mm enters the circular tissue parallel to the z direction. The propagation path of each photon is calculated from the scattering coefficient, assuming the absorption is negligible. An MC simulation of photon migration within irradiated tissues was built[20,21] in order to calculate the full scattering profile at all possible exit angles. This simulation is based on the assumption that all photons reaching the tissue begin as ballistic photons. Given the current photon's direction (θ_{old}) and that the probability of a photon to scatter is $[1 - \exp(-\mu_s dr)]$, if the photon scattered, its new direction (θ_{new}) was calculated using

$$\theta_{\text{new}} = \theta_{\text{old}} + s\ \cos(g), \tag{1}$$

where s is a random number from the group $(-1,1)$. Hence, the additional scattering angle is uniformly distributed. This process is repeated until the photon exits the tissue, and then its location is saved. This simulation approach has been validated by experimental measurements.[11]

Several repetitions of the simulation for each tissue diameter (5, 10, and 15 mm) were held to determine the variations in the maximum intensity (value and exit angle) due to the change in the reduced scattering coefficient $\mu_s' = \mu_s(1 - g)$. The values of the μ_s' were in the range of the human skin values of 2 to 26 cm^{-1}.[24–26]

2.2 *Two-Dimensional Model of Circular Scattering and Absorbing Tissue*

In order to determine the role of absorption on the full scattering profile, the model described in Sec. 2.1 was repeated while incorporating the absorption coefficient μ_a thus, the propagation path of each photon is calculated from two values of μ_s' (18 and 26 cm^{-1}) while changing the μ_a between 0 to 0.3 cm^{-1}. First, the full scattering profile was examined for different μ_a while maintaining the same μ_s'. Next, the intensity of the isobaric point and the maximum of the full scattering profile were extracted and presented as a function of μ_a.

2.3 *Three-Dimensional Model of Cylindrical Tissue*

A three-dimensional (3-D) model of a cylinder of tissue was created with the same method and properties as described in the 2-D model [Fig. 1(b)]. Ten repetitions of the 3-D MC simulation[11,20,21] were built in order to calculate the full scattering profile at all possible exit angles. The illumination was set to be a square of 1.5×1.5 mm^3, and the transmitted photons were collected from a 1-mm thick slice [gray area in Fig. 1(b)] along the cylinder surface. As in 2-D, simulations for two tissue diameters (4 and 15 mm) were held to determine the variations of the maximal intensity of the full scattering profile (value and exit angle) due to the change in the reduced scattering coefficient. Furthermore, μ_a (between 0 and 0.3 cm^{-1}) was added in order to examine its influence on the full scattering profile.

3 Results

3.1 *Maximal Measurement Point*

First, the 2-D simulation described in Sec. 2.1 was performed. After obtaining the full scattering profile [see example in Fig. 2(a)], as previously published,[21] one may notice that for

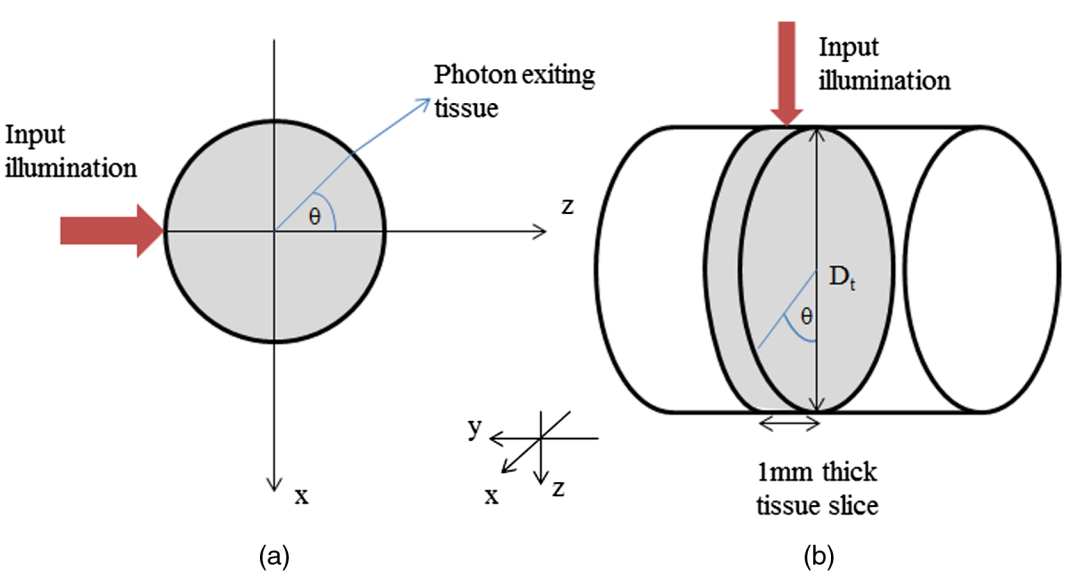

Fig. 1 Schema of tissue model: (a) two-dimensional (2-D) circular tissue and (b) three-dimensional (3-D) cylindrical tissue.

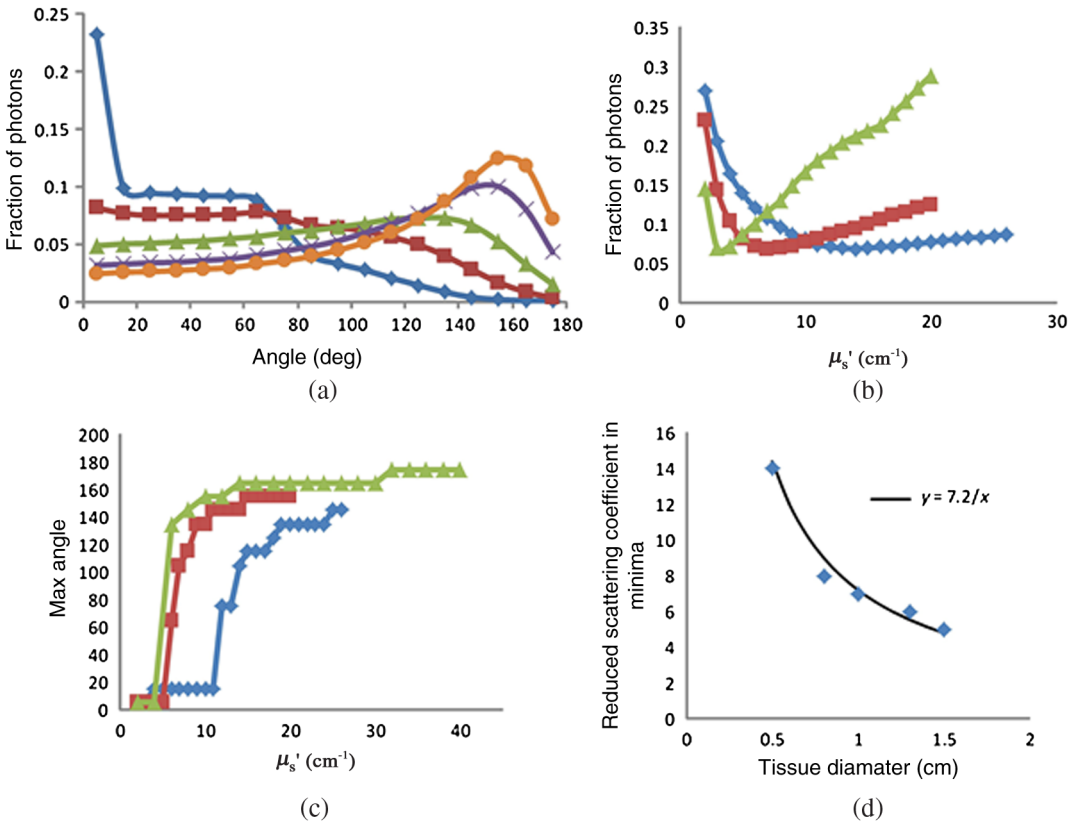

Fig. 2 Defining multiple scattering region: (a) example of full scattering profile of 10-mm circular tissue for different reduced scattering coefficients (diamonds, squares, triangles, x's, and circles indicate 2, 5, 9, 15, and 20 cm^{-1}, respectively); (b) value of maximum intensity of full scattering profile; and (c) its angular position versus reduced scattering coefficient. The tissue diameter is 5 mm (diamonds), 10 mm (squares), and 15 mm (triangles). (d) Relation between reduced scattering coefficient in which the maximum intensity is at its minimal value and tissue diameter.

a low μ_s' the maximum is received in low angles (i.e., transmission) and as the μ_s' increases, the maximum value transfers to higher angles (i.e., reflection). The maximum value [the standard deviation (STD) was less than 2% for all experiments] of the full scattering profile [Fig. 2(b)] and its exit angle [Fig. 2(c)] for different μ_s' was collected for three tissue diameters (diamonds, squares, and triangles represent 5, 10, and 15 mm, respectively). The value of this maximum alternates from high to low and to high again [Fig. 2(b)], and its extreme point is reached when the exit angle is 90 deg. Furthermore, the μ_s' in which the exit angle is 90 deg decreases as the tissue diameter increases. Only farther away from this extreme point do we enter the multiple scattering region, as we will demonstrate later on. The μ_s' of the extreme point was found to be inversely related to the tissue diameter [Fig. 2(d)].

The 3-D simulation described in Sec. 2.3 was performed in order to verify these findings in a tissue diameter of 4 mm. As in 2-D, the value (STD < 2%) of this maximum of the full scattering profile alternated from high to low and to high [Fig. 3(a)] and its extreme point is reached when the exit angle is 90 deg [Fig. 3(b)]. Note that the steep jump in Fig. 3(b) is a result of the numerical accuracy and has no physical meaning.

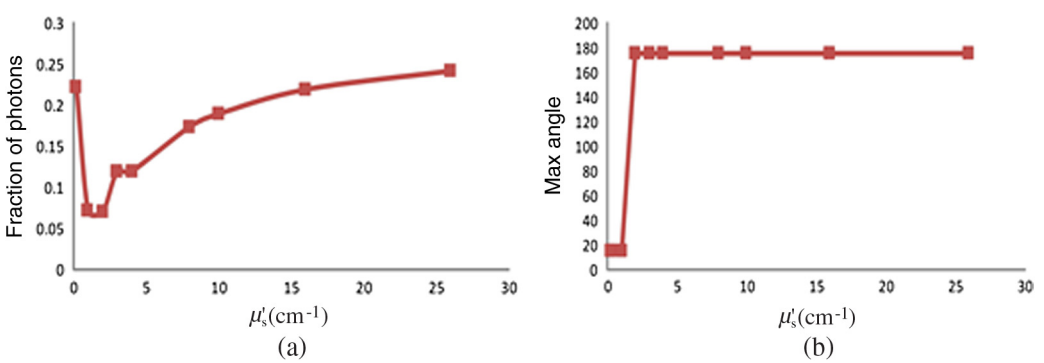

Fig. 3 (a) Maximum intensity (b) and its position in full scattering profile versus reduced scattering coefficient in 3-D simulation of 4 mm diameter cylindrical tissue.

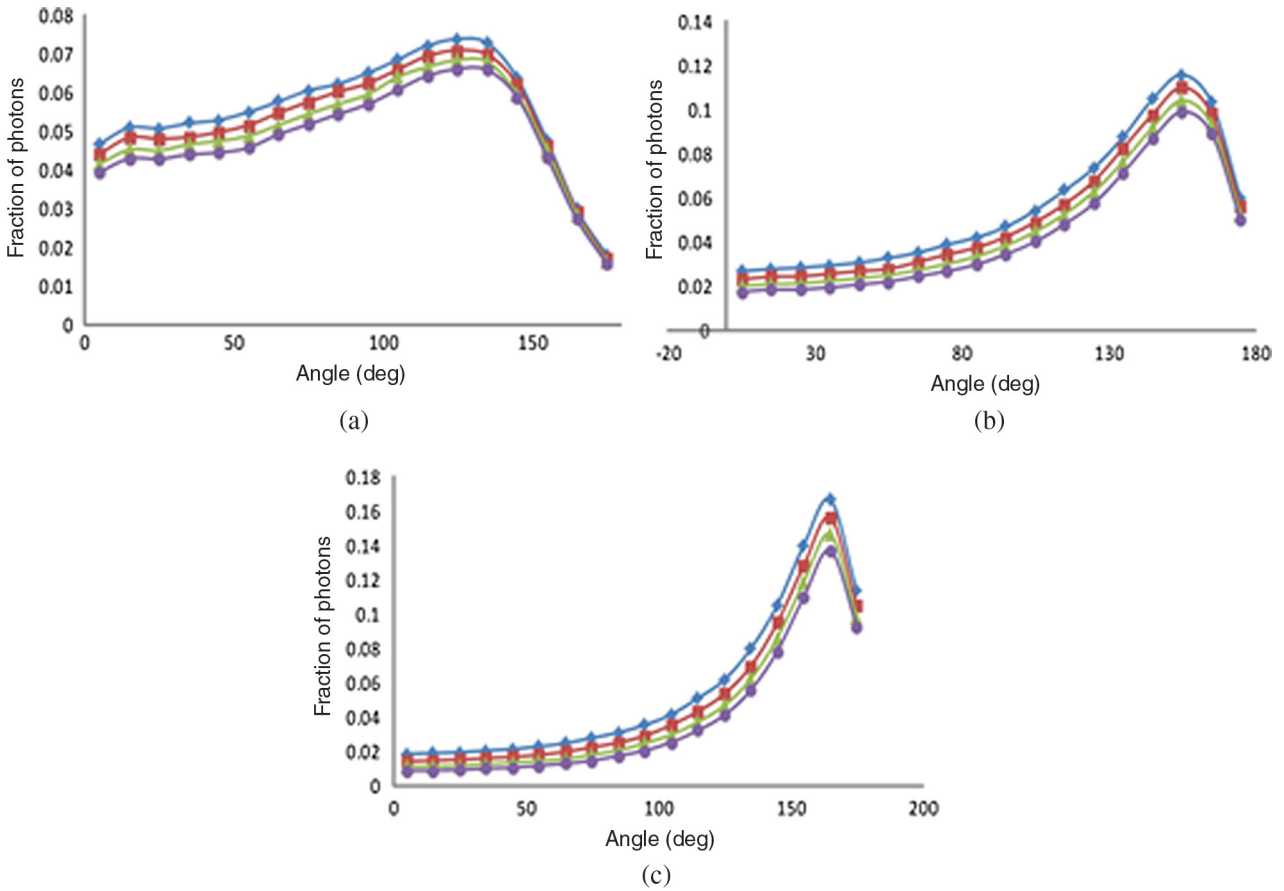

Fig. 4 Full scattering profile for a reduced scattering coefficient of 18 cm^{-1} and different absorption coefficients (diamonds, squares, triangles, and circles indicate 0, 0.1, 0.2, and 0.3 cm^{-1}, respectively). The tissue diameters are: (a) 5 mm, (b) 10 mm, and (c) 15 mm.

3.2 *Influence of Absorption and Multiple Scattering on Full Scattering Profile*

The 2-D simulation described in Sec. 2.2 was performed in order to investigate the influence of absorption on the full scattering profile, which was previously[20,21] ignored. First, the full scattering profile (STD < 2%) for the same reduced scattering coefficient (18 cm^{-1}) and different absorption coefficients (0 to 0.3 cm^{-1}) was examined in different tissue diameters [5, 10, and 15 mm, respectively in Figs. 4(a)–4(c)]. As expected, the full scattering profile is attenuated but unchanged in shape. Next, the position of the isobaric point was tested under different absorption coefficients [0, 0.1, and 0.3 cm^{-1}, respectively in Figs. 5(a)–5(c)]. As expected, the angle of the isobaric point is unchanged, and its value (fraction of photons) decreases (STD < 2%).

In order to further investigate the attenuation due to absorption, the value of the maxima (solid lines) and the isobaric point (dashed lines) were examined (STD < 2%), for two reduced scattering coefficients [Fig. 6(a)]. It was found that the values of both the maxima and isobaric point linearly decrease in relation to the absorption coefficient. Next, the 3-D simulation described in Sec. 2.3 with a tissue diameter of 15 mm [Fig. 6(b)] was performed. As in the 2-D simulation, the value of the maxima (solid lines) and the isobaric (dashed lines) point linearly decreased (STD < 3%) with the absorption coefficient for different reduced scattering coefficients [diamonds and squares indicate 2 and 10 cm^{-1}, respectively in Fig. 6(b)].

4 Discussion

In this work, we have investigated the influence of absorption and multiple scattering on the full scattering profile in different tissue diameters in 2-D as well as in 3-D simulations. In both of these sets of simulations, a simplistic uniformly distributed phase function was used as opposed to the typical phase functions, such as the Henyey–Greenstein phase function.[27,28] We chose this distribution since our purpose was not to reconstruct optical properties from experimental data, but rather to find the isobaric point from predetermined optical properties. Furthermore, the use of this phase function for simulation has been validated by experimental measurements.[11] We have shown that the maximal intensity alternates from high (corresponding to transmission) to low and to high (corresponding to reflection) again as the reduced scattering coefficient increases [Fig. 2(b)]. This is expected since for low reduced scattering coefficients most of the light is transmitted through the tissue without interruptions. As the reduced scattering coefficient increases the light is scattered to a broader range of angles. For very high reduced scattering coefficients most of the light is reflected directly back to the source. Furthermore, the value of this intensity is minimal for an exit angle of 90 deg. We have used this in order to define the conditions for multiple scattering. When the scattering is much higher than the inverse diameter, the path of the light in the tissue becomes significantly longer. As Fig. 2 shows if the tissue diameter is small enough, the assumption of multiple scattering is not

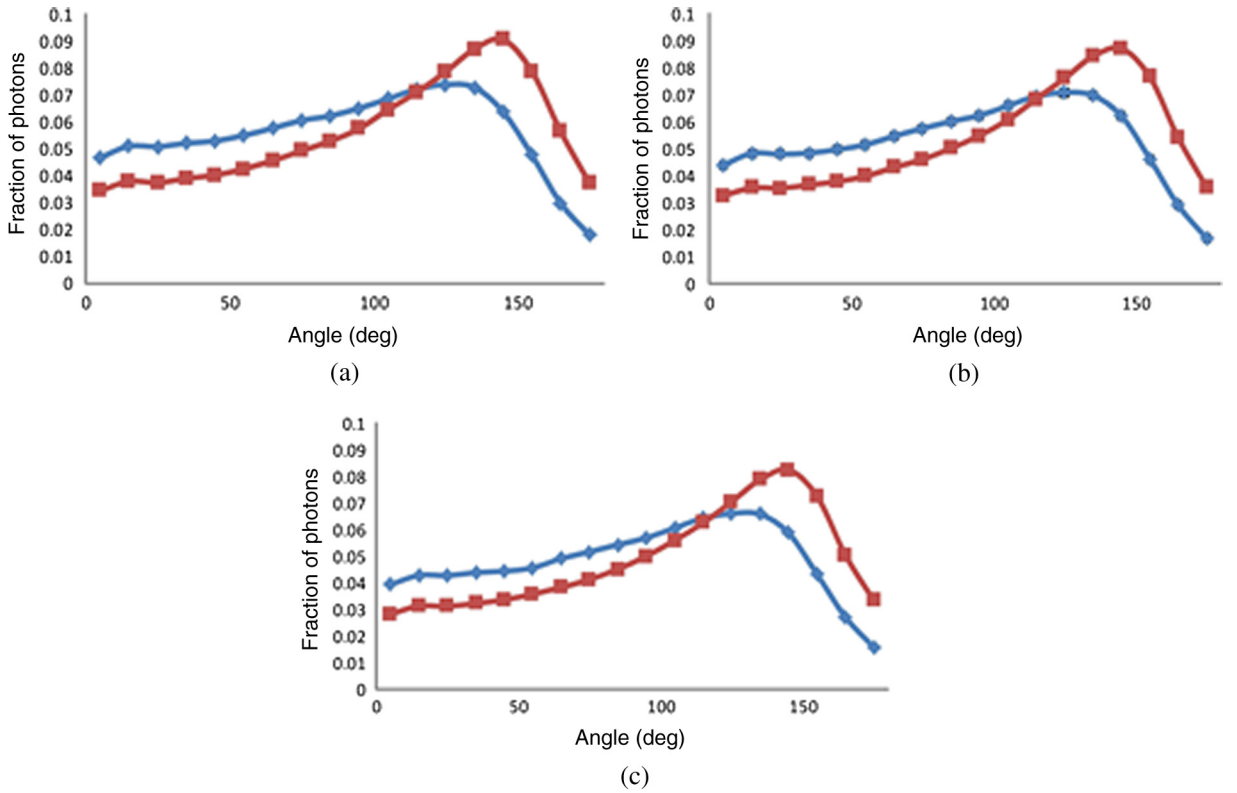

Fig. 5 Position of isobaric point for different absorption coefficients (18 and 26 are marked by diamond and squares, respectively) for a tissue diameter of 5 mm. Absorption coefficients are: (a) 0, (b) 0.1, and (c) 0.3 cm^{-1}.

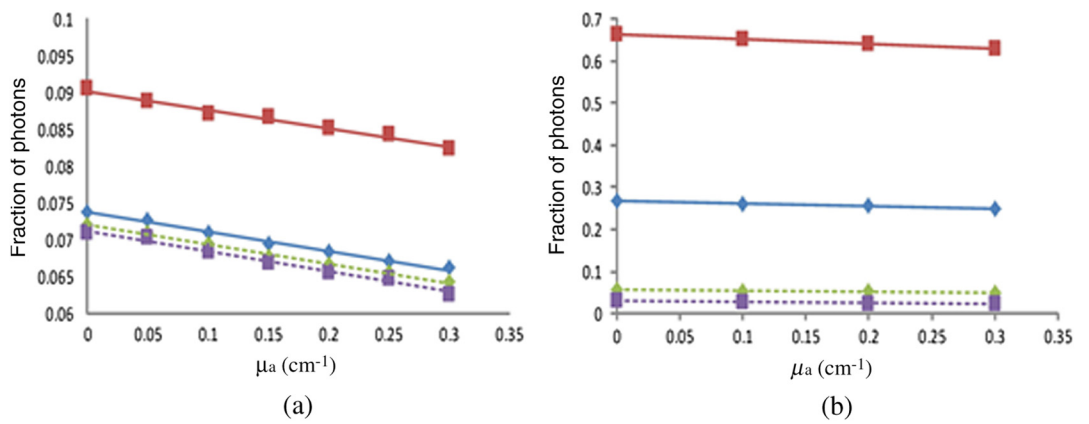

Fig. 6 The change in maximum intensity (solid lines) and intensity in isobaric point (dashed lines) versus absorption coefficient. Two representative reduced scattering coefficients where chosen: (a) 18 cm^{-1} (diamonds) and 26 cm^{-1} (squares) in 2-D simulation for a tissue diameter of 5 mm and (b) 2 cm^{-1} (diamonds) and 10 cm^{-1} (squares) in 3-D simulation for a tissue diameter of 15 mm.

Table 1 Comparison of two-dimensional slopes between scattering [from Fig. 6(a)] and multiple scattering [from Fig. 7(b)]. A tissue diameter of 5 mm represents scattering and a diameter of 15 mm represents multiple scattering.

	5 mm		15 mm		
μ_s' (cm^{-1})	18	26	10	18	40
Isobaric point	0.026	0.028	0.075	0.088	0.081
Maximum point	0.026	0.027	0.070	0.098	0.132

Table 2 Three-dimensional slopes [from Fig. 6(b)] for the case of multiple scattering (tissue diameter is 15 mm).

μ_s' (cm^{-1})	2	10
Isobaric point	0.029	0.028
Maximum point	0.059	0.111

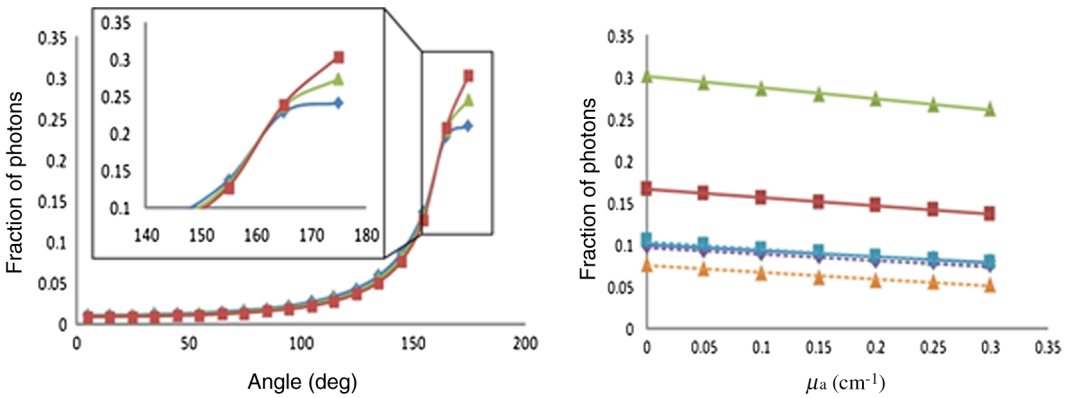

Fig. 7 2-D simulation of multiple scattering for a tissue diameter of 15 mm. (a) Full scattering profile for different reduced scattering coefficients (32, 36, and 40 cm^{-1} indicate to diamonds, triangles, and squares, respectively). (b) The change in maximum intensity (solid lines) and intensity in isobaric point (dashed lines) versus absorption coefficient. Three representative reduced scattering coefficients where chosen: 10 cm^{-1} (diamonds), 18 cm^{-1} (squares), and 40 cm^{-1} (triangles).

true and hence, the influence of absorption should be taken into consideration accordingly.

We have previously discussed an isobaric point which is indifferent to changes in the reduced scattering coefficient.[20] However, as mentioned before, this point only exists in a certain range of reduced scattering coefficients. For example, in a 2-D simulation of a 10-mm circular tissue [Fig. 2(a)], one may notice that the isobaric point which exists for reduced scattering coefficients of 15 and 20 cm^{-1} (exes and circles), is not the same as with reduced scattering coefficients for 2, 5, and 9 cm^{-1} (diamonds, squares, and triangles). Figure 2(b) sheds new light on this phenomenon. Only when we cross the extreme point and enter the linear region does the isobaric point exist.

We have shown that although the intensity linearly attenuates as a result of absorption, the dependency of intensity on the absorption coefficient depends on multiple scattering.

In the first 2-D simulation of a 5-mm diameter tissue, the slopes of the linear fit were extracted [from Fig. 6(a)] in order to examine the linear dependency (Table 1). It was found that the values of both maxima and isobaric point linearly decrease according to the absorption coefficient with the same slope (0.026 ± 0.001). However, when performing the 3-D simulation with a tissue diameter of 15 mm [Fig. 6(b)], some differences were found. In the isobaric point (dashed lines), the slope of the linear ratio was similar (0.028 ± 0.001, see Table 2) for different reduced scattering coefficients [diamonds and squares indicate 2 and 10 cm^{-1}, respectively in Fig. 6(b)]. However, the slopes (Table 2) of the maxima (solid lines) were different (0.059 and 0.1112 corresponding to 2 and 10 cm^{-1}, respectively). This phenomenon can be explained by multiple scattering. Once multiple scattering occurs, the path of the photon in the tissue increases significantly with respect to the reduced scattering coefficient. Hence, higher scattering will accumulate stronger absorption losses [as was presented in Fig. 6(b)]. This is not only the case in 3-D, but rather whenever the reduced scattering coefficient is high with respect to the tissue diameter. A 2-D example of multiple scattering is presented for a tissue diameter of 15 mm [Figs. 7(a) and 7(b)]. Though the slope (Table 1) of the isobaric point (dashed lines) remains the same (0.07 ± 0.01) for different reduced scattering coefficients, the slope of the maxima point increases according to the reduced scattering coefficients (0.070, 0.098, and 0.132 in respect to 10, 18, and 40 cm^{-1}) [solid line in Fig. 7(b)].

5 Conclusions

In this work, we have investigated the influence of absorption and multiple scattering on the full scattering profile in different tissue diameters in 2-D as well as in 3-D simulations. The findings of this work demonstrate a realistic model for optical tissue measurements such as PPG for calculation of arterial oxygen saturation and heart rate.[23] A cylindrical tissue with varying diameters between 4 and 15 mm was simulated since this the typically studied region in PPG is the fingertip (about 10 to 15 mm diameter) or earlobe (about 5 mm diameter).

The dependence of intensity on the absorption coefficients remains constant for all intensity points of the full scattering profile and scattering coefficients in regular scattering, while this is not the case in multiple scattering. When entering the multiple scattering regime, the dependence of intensity on absorption coefficients may vary. We have shown that although this variation occurs for the maximal intensity point (as an example), the isobaric point maintains a constant dependence. This phenomenon reinforces the advantage of measuring the isobaric point, which is also not influenced by changes in the scattering coefficient. By taking both absorption and multiple scattering under consideration, we demonstrated a more realistic model for optical tissue measurement. These findings can be implemented on methods such as NIR spectroscopy, PPG experiments, and analyzing exact oxygen saturation values. However, further investigation is needed in order to define the exact limit at which multiple scattering begins.

References

1. J. Allen, "Photoplethysmography and its application in clinical physiological measurement," *Physiol. Meas.* **28**(3), R1–R39 (2007).
2. V. Tuchin, "Optical properties of tissues with strong (multiple) scattering," in *Tissue Optics: Light Scattering Methods and Instruments for Medical Diagnosis*, V. Tuchin, Ed., pp. 1–15, SPIE Press, Bellingham, Washington (2007).

3. S. L. Jacques, "Optical properties of biological tissues: a review," *Phys. Med. Biol.* **58**(11), R37–R61 (2013).
4. A. C. Boccara and P. M. W. French, "Towards optical biopsy: a brief introduction," in *Waves and Imaging Through Complex Media*, P. Sebbah, Ed., Springer, Netherlands (2001).
5. F. Helmchen and W. Denk, "Deep tissue two-photon microscopy," *Nat. Methods* **2**, 932–940 (2005).
6. M. Heckmeier et al., "Imaging of dynamic heterogeneities in multiple-scattering media," *J. Opt. Soc. Am. A* **14**(1), 185–191 (1997).
7. D. A. Boas, L. E. Campbell, and A. G. Yodh, "Scattering and imaging with diffusing temporal field correlations," *Phys. Rev. Lett.* **75**(9), 1855–1859 (1995).
8. S. L. Jacques and B. W. Pogue, "Tutorial on diffuse light transport," *J. Biomed. Opt.* **13**(4), 041302 (2008).
9. C. Balas, "Review of biomedical optical imaging—a powerful, non-invasive, non-ionizing technology for improving *in vivo* diagnosis," *Meas. Sci. Technol.* **20**(10), 10402001–10402012 (2009).
10. B. J. Tromberg et al., "Assessing the future of diffuse optical imaging technologies for breast cancer management," *Med. Phys.* **35**(6), 2443–2451 (2008).
11. R. Ankri et al., "*In-vivo* tumor detection using diffusion reflection measurements of targeted gold nanorods–a quantitative study," *J. Biophotonics* **5**(3), 263–273 (2012).
12. R. Vered, S. Havlin, and H. Taitelbaum, "Optical detection of hidden tumors," *Proc. SPIE* **2389**, 851–858 (1995).
13. L. Wang and S. L. Jacques, "Hybrid model of Monte Carlo simulation and diffusion theory for light reflectance by turbid media," *J. Opt. Soc. Am. A* **10**(8), 1746–1752 (1993).
14. L. Wang, S. L. Jacques, and L. Zheng, "MCML–Monte Carlo modeling of light transport in multi-layered tissues," *Comput. Methods Programs Biomed.* **47**(2), 131–146 (1995).
15. R. Ankri, H. Taitelbaum, and D. Fixler, "Reflected light intensity profile of two-layer tissues: phantom experiments," *J. Biomed. Opt.* **16**(8), 085001 (2011).
16. D. Fixler and R. Ankri, "Subcutaneous gold nanorod detection with diffusion reflection measurement," *J. Biomed. Opt.* **18**(6), 061226 (2013).
17. R. A. J. Groenhuis, A. H. Ferweda, and J. J. Ten Bosch, "Scattering and absorption of turbid materials determined from reflection measurements. 1: theory," *Appl. Opt.* **22**(16), 2456–2462 (1983).
18. D. Jakubowski et al., "Quantitative absorption and scattering spectra in thick tissues using broadband diffuse optical spectroscopy," Chapter 12 in *Biomedical Optical Imaging*, J. G. Fujimoto and D. L. Farkas, Eds., pp. 330–355, Oxford University Press, New York (2009).
19. T. H. Pham et al., "Broad bandwidth frequency domain instrument for quantitative tissue optical spectroscopy," *Rev. Sci. Instrum.* **71**(6), 2500–2513 (2000).
20. H. Duadi, R. Popovtzer, and D. Fixler, "The dependence of light scattering profile in tissue on blood vessel diameter and distribution–a computer simulation study," *J. Biomed. Opt.* **18**(11), 111408 (2013).
21. H. Duadi, I. Feder, and D. Fixler, "Linear dependency of full scattering profile isobaric point on tissue diameter," *J. Biomed. Opt.* **19**(2), 026007 (2014).
22. J. E. Sinex, "Pulse oximetry: principles and limitations," *Am. J. Emerg. Med.* **17**(1), 59–66 (1999).
23. K. H. Shelley, "Photoplethysmography: beyond the calculation of arterial oxygen saturation and heart rate," *Anesth. Analg.* **105**(6), S31–S36 (2007).
24. T. Lister, P. A. Wright, and P. H. Chappell, "Optical properties of human skin," *J. Biomed. Opt.* **17**(9), 090901 (2012).
25. A. N. Bashkatov et al., "Optical properties of human skin, subcutaneous and mucous tissues in the wavelength range from 400 to 2000 nm," *J. Phys. D Appl. Phys.* **38**(15), 2543–2555 (2005).
26. L. Zhang, A. Shi, and H. Lu, "Determination of optical coefficients of biological tissue from a single integrating-sphere," *J. Mod. Opt.* **59**(2), 121–125 (2012).
27. M. Hammer, A. N. Yaroslavsky, and D. Schweitzer, "A scattering phase function for blood with physiological haematocrit," *Phys. Med. Biol.* **46**(3), N65–N69 (2001).
28. A. N. Yaroslavsky et al., "Influence of the scattering phase function approximation on the optical properties of blood determined from the integrating sphere measurements," *J. Biomed. Opt.* **4**(1), 47–53 (1999).

Hamootal Duadi received her BSc degree in electrical engineering from Bar-Ilan University in 2006. She completed her direct PhD studies in Bar-Ilan University 2011. She specialized in optical information processing, super resolution, diffractive optical elements and beam shaping, 3-D and range estimation. Her current research fields are pulse oximetry, light-tissue interaction, and live cell imaging.

Dror Fixler received his PhD degree from the Department of Physics, Bar-Ilan University, Israel, in 2003. He is a member of the Faculty of Engineering and the Nano Center of Bar-Ilan University. He has published over 50 original research papers and holds over 10 issued patents. His research interests include fluorescence measurements (FLIM and anisotropy decay), optical super resolution, high-end electro-optical system engineering and light-tissue interactions. He received several international awards and presented at over 20 international conferences.